Qi Lin (Orcid ID: 0000-0002-2902-4917)

zheng yanling (Orcid ID: 0000-0002-8041-2843)

Hou Lijun (Orcid ID: 0000-0002-5001-1707)

Yin Guoyu (Orcid ID: 0000-0002-8949-3731)

Liu Min (Orcid ID: 0000-0001-6515-5095)

Title: Potential response of dark carbon fixation to global warming in estuarine and coastal waters

Running Title: Effects of warming on dark carbon fixation

Lin Qi[1,2] (0000-0002-2902-4917), Yanling Zheng[1,2,3,4,*] (0000-0002-8041-2843), Lijun Hou[3,*] (0000-0002-5001-1707), Bolin Liu[3] (0000-0002-4964-0987), Jie Zhou[3] (0000-0003-1631-0882), Zhirui An[1,2] (0000-0001-6357-1802), Li Wu[1,2] (0000-0002-9999-7167), Feiyang Chen[3] (0000-0003-0582-7333), Zhuke Lin[1,2] (0009-0006-1407-4803), Guoyu Yin[1,2,4] (0000-0002-8949-3731), Hongpo Dong[3] (0000-0003-4940-2943), Xiaofei Li[3] (0000-0002-3785-0741), Xia Liang[3] (0000-0003-3882-5406), Min Liu[1,2,4] (0000-0001-7672-7482)

[1]School of Geographic Sciences, East China Normal University, Shanghai 200241, China

[2]Key Laboratory of Geographic Information Science (Ministry of Education), East

This article has been accepted for publication and undergone full peer review but has not been through the copyediting, typesetting, pagination and proofreading process which may lead to differences between this version and the Version of Record. Please cite this article as doi: 10.1111/gcb.16702

China Normal University, Shanghai 200241, China

[3]State Key Laboratory of Estuarine and Coastal Research, Yangtze Delta Estuarine Wetland Ecosystem Observation and Research Station, Ministry of Education & Shanghai, East China Normal University, Shanghai 200241, China

[4]Key Laboratory of Spatial-temporal Big Data Analysis and Application of Natural Resources in Megacities, Ministry of Natural Resources, Shanghai 200241, China

*Corresponding authors:

Yanling Zheng (ylzheng@geo.ecnu.edu.cn)

Postal address: School of Geographic Sciences, East China Normal University, 500 Dongchuan Road, Minhang District, Shanghai 200241, China

Lijun Hou (ljhou@sklec.ecnu.edu.cn)

Postal address: State Key Laboratory of Estuarine and Coastal Research, East China Normal University, 500 Dongchuan Road, Minhang District, Shanghai 200241, China

Abstract: Dark carbon fixation (DCF), through which chemoautotrophs convert inorganic carbon to organic carbon, is recognized as a vital process of global carbon biogeochemical cycle. However, little is known about the response of DCF processes in estuarine and coastal waters to global warming. Using radiocarbon labelling method, the effects of temperature on the activity of chemoautotrophs were investigated in benthic water of the Yangtze estuarine and coastal areas. A dome-shaped thermal response pattern was observed for DCF rates (i.e., reduced rates at lower or higher temperatures), with the optimum temperature (T_{opt}) varying from about 21.9 °C to 32.0 °C. Offshore sites showed lower T_{opt} values and were more vulnerable to global warming compared with nearshore sites. Based on temperature seasonality of the study area, it was estimated that warming would accelerate DCF rate in winter and spring but inhibit DCF activity in summer and fall. However, at an annual scale, warming showed an overall promoting effect on DCF rates. Metagenomic analysis revealed that the dominant chemoautotrophic carbon fixation pathways in the nearshore area were Calvin-Benson-Bassham (CBB) cycle, while the offshore sites were co-dominated by CBB and 3-hydroxypropionate/4-hydroxybutyrate (3-HP/4-HB) cycles, which may explain the differential temperature response of DCF along the estuarine and coastal gradients. Our findings highlight the importance of incorporating DCF thermal response into biogeochemical models to accurately estimate the carbon sink potential of estuarine and coastal ecosystems in the context of global warming.

Keywords: Dark carbon fixation; Temperature response; Estuary; Coast; Benthic water;

Chemoautotrophy; Global warming

1. Introduction

Dark carbon fixation (DCF), as an important carbon sink process, has long been ignored in estuarine and coastal carbon cycles compared with photoautotrophic carbon fixation (Baltar et al., 2016; Zhou et al., 2017). DCF is mainly carried out by chemoautotrophs, which typically thrive near the interfaces between reductive and oxidizing environments, such as the chemoclines in water bodies or the aerobic-anoxic transition zones in sediments (Jørgensen, 1982; Labrenz et al., 2005), obtaining metabolic energy by oxidizing various reductive inorganic substrates [e.g., hydrogen (H_2), ammonia (NH_3), nitrite (NO_2^-), hydrogen sulfide (H_2S), sulfur (S), thiosulfate ($S_2O_3^{2-}$) and ferrous iron (Fe^{2+})]. Using these energy, organic molecules are synthesized from dissolved inorganic carbon (DIC) by chemoautotrophs, which is now recognized to rival the importance of photosynthesis in the global carbon cycle (Bräuer et al., 2013; Guerrero-Feijoo et al., 2018).

Seven pathways of DCF, including Calvin-Benson-Bassham (CBB) cycle, 3-hydroxypropionate/4-hydroxybutyrate (3-HP/4-HB) cycle, reductive tricarboxylic acid (rTCA) cycle, 3-hydroxypropanoate (3-HP) bicycle, reductive acetyl-CoA (WL) pathway, dicarboxylate/4-hydroxybutyrate (DC/4-HB) cycle and reductive glycine pathway, have currently been found in chemoautotrophs (Berg, 2011; Figueroa et al., 2018; Hügler & Sievert, 2010). Among them, CBB cycle, 3-HP/4-HB cycle, and rTCA cycle are the most important chemoautotrophic DCF pathways known in various

habitats, such as freshwater lakes (Alfreider et al., 2017), deep-sea (Berg, 2011) and hydrothermal vent systems (Hügler & Sievert, 2010). During CBB cycle, Ribulose 1,5-bisphosphate (RuBP) carboxylase/oxygenase (RubisCO) catalyses the key reaction by which inorganic carbon may be assimilated into organic carbon (OC). Among the four RuBisCO forms, form I and form II are known to participate in prokaryotic autotrophy (Berg, 2011), and *cbbL* (encoding form I RuBisCO) and *cbbM* (encoding form II RuBisCO) are the most representative marker genes (Alfreider et al., 2017). In addition, more energy-efficient pathways alternative to the CBB cycle are employed by microbes (Bar-Even et al., 2012; Hügler & Sievert, 2010). For the 3-HP/4-HB cycle, the key enzyme acetyl-CoA carboxylase (ACCase) is encoded by *accA* gene (Yakimov et al., 2011) and the 4-hydroxybutyryl-CoA dehydratase is encoded by *hbd* gene (Alfreider et al., 2017). During the rTCA cycle, the large subunit of the ATP-dependent citrate lyase (ACL) is encoded by *aclB* gene (Takai et al., 2005). Temperature is recognized as a primary factor regulating microbial metabolic activities (Walker et al., 2018; Zheng et al., 2020). However, knowledge about the potential effect of global warming on DCF remains poorly understood, especially for habitats having high DCF rates, such as estuaries and coasts (Signori et al., 2017).

Estuarine and coastal ecosystems exhibit extremely active redox reactions due to the influence of periodic exposure and inundation under tidal action and a large amount of anthropogenic nutrient substrates input (Liu et al., 2022). Chemoautotrophic carbon

fixation in estuarine and coastal zones is estimated at approximately 328 Tg C y^{-1}, which represents approximately 42.6% of oceanic DCF production (Middelburg, 2011). However, these complex environments appear to be the frontline of global warming due to the influence of various complex factors (Belkin, 2009; Zheng et al., 2020). Data from a twelve-year (2007-2019) monitoring study of 166 estuaries along the Australian coastline showed that estuary temperature increased at a rate of 0.2 °C $year^{-1}$, which was an order of magnitude faster than predicted by global ocean models (Scanes et al., 2020). Based on remote sensing data from 1982 to 2017, surface water temperature in the Yangtze Estuary was estimated to increase at a rate of about 0.05 °C $year^{-1}$, which was significantly greater than that of the open sea (Wang et al., 2021). These higher warming rates in estuarine waters may be attributed to their shallow depth which can provide a greater capacity to absorb radiative heat per volume of water (Scanes et al., 2020). Therefore, it is of great importance to predict how DCF capacity responds to temperature increase in these carbon sequestration hotspots. Previous study showed that DCF rates were positively correlated with temperature through the water column in the Atlantic off the Galician coast (Guerrero-Feijoo et al., 2018). However, limited field studies in marine environments have given inconsistent results that DCF rates were negatively correlated with (Garcia-Cantizano et al., 2005; Reinthaler et al., 2010; Zhou et al., 2017) or insensitive to temperature increases (Kyewalyanga et al., 2007; Scranton et al., 2020). Nevertheless, those temperature response patterns of DCF rate were

comprehensive effect of the complex environments, which may be strongly affected by microbial dynamics and physicochemical properties of waters at different depths. Therefore, it is still urgent to reveal the potential effect of global warming on DCF in estuarine and coastal waters.

The objectives of this study are (i) to identify the temperature response pattern of DCF in the complex estuarine and coastal waters; (ii) to simulate the response of DCF capacity to different warming scenarios; and (iii) to reveal the response mechanism of DCF to global warming in estuarine and coastal waters. This study provides an important scientific basis for more accurate quantitative assessment of estuarine and coastal net carbon sequestration capacity in the context of climate change.

2. Materials and Methods

2.1 Study area and field sampling

The Yangtze River, the largest river of China, annually transports a runoff of 885 billion m^3 with approximately 86 million tons of sediments to the estuary and adjacent areas in recent ten years (Sun et al., 2022). Intensive mixing of freshwater and seawater generally creates a steep environmental gradient in the Yangtze Estuary (Zheng et al., 2016). In addition, the study area is largely impacted by complex hydrology, physical dynamics and anthropogenic processes, which represents an ideal estuary-coast continuum system across the globe. The annual temperature range of the study area

generally ranges from about 6.3 to 27.9 °C (Table S1). Field surveys and sample collection were conducted along the environmental gradient of the Yangtze Estuary and its adjacent coastal areas during the October cruise of National Natural Science Foundation of China (NSFC) in 2021 (Figure 1). Water samples were collected near the bottom of the euphotic zone with vibrant redox reaction activity (Bräuer et al., 2013) using a conductivity-temperature-depth (CTD) rosette fitted with 12-L Niskin bottles. At each sampling site, 30 L of water was collected and stored in the dark under 4 °C for DCF rate measurement and temperature manipulation experiments, and 100 ml of water were filtered with 0.45 μm pore-size sterile filters (Waterman) for measurement of environmental parameters including DIC, chlorophyll a (Chl-a), ammonium (NH_4^+), NO_2^-, nitrate (NO_3^-), phosphate (PO_4^{3-}), silicate (SiO_4^{3-}), dissolved organic carbon (DOC) and total dissolved nitrogen (TDN). Meanwhile, known amounts of water samples were also immediately filtered with 0.22 μm pore-size sterile filters (Waterman), and the membranes were carefully preserved at -20 °C for later molecular analyses.

2.2 Measurement of environmental parameters

Water depth and salinity were measured with a CTD profiler. Dissolved oxygen (DO) was measured *in situ* by an oxygen sensor (OX500, Unisense, Denmark) and pH was measured with pH meter (Mettler-Toledo). Nutrients including NH_4^+, NO_2^-, NO_3^-,

PO_4^{3-} and SiO_4^{3-} were measured spectrophotometrically on a continuous flow analyzer (SAN Plus, Skalar Analytical B.V., the Netherlands). Chl-a was measured on discrete water samples using the in vitro fluorometric method with 90% acetone extraction and determined on a Turner Designs TD-700 fluorometer (Giese, 1994). DIC, DOC and TDN were determined using a TOC/TN-Analyzer (TOC-5000, Shimadzu, Kyoto, Japan). The environmental characteristics in this study are shown in Table S2.

2.3 Measurement of dark carbon fixation rates

Water DCF rates were determined using ^{14}C sodium bicarbonate (specific activity, 50 μCi/mL; Perkin-Elmer, USA) (Alonso-Saez et al., 2010). For each sample (40 mL), 3 replicates and one killed control were analyzed. Killed controls were preserved with formaldehyde (4.4%, final conc.) prior to bicarbonate addition. Samples were added with 20 μl $NaH^{14}CO_3$ solution (0.025 μCi/mL, final conc.) and incubated in the dark for 24 h under different temperatures in thermostat-controlled incubators. In the present study, we applied a temperature gradient ranging from 5 to 40 °C at 5 °C intervals, considering the seasonal fluctuation of temperature in the study area. After incubation, each sample was added with 5 mL formaldehyde and filtered with 0.22 μm polycarbonate membrane (Millipore). The membrane was put into a scintillation vial and exposed to concentrated HCl fume overnight. Scintillation cocktail (Fisher Scientific, Scintiverse BD cocktail SX18-4) was added to each vial (5 mL) and placed

in the dark for 18 h, until the radioactivity of the filters was counted with the liquid scintillation counter (300SL, Hidex, USA). The disintegrations per minute (DPM) of the formalin-fixed blank were subtracted from the samples, and the resulting DPM were converted into ^{14}C incorporation rates. The calculation formula is as follows (Liu et al., 2022):

$$R_{DCF} = \frac{DPM_{inc} \times DIC \times 1.05}{DPM_0 \times t}$$

where DPM_{inc} is the difference between the radioactivity in the water samples and control blanks; DIC is the dissolved inorganic C concentration of the water sample; 1.05 is the isotope coefficient used for correcting the uptake of ^{14}C, since the uptake of ^{14}C is 5% lower than that of ^{12}C (Molari et al., 2013); DPM_0 is the activity of all the ^{14}C added; t is the incubation time.

2.4 DNA extraction and quantitative PCR (Q-PCR)

Total environmental DNA was extracted by using the DNeasy PowerWater Kit (QIAGEN, Germany) in accordance with the instruction of the manufacturer. The quality and concentration of the extracted DNA were measured with a Nanodrop Spectrophotometer ND-2000 (Thermo Fisher Scientific, USA). Q-PCR was then conducted based on the total environmental genomic DNA of *in situ* water to measure the abundance of *cbbL* and *cbbM* genes of CBB cycle, *accA* and *hbd* genes of 3-HP/4-HB cycle, and *aclB* gene of rTCA cycle (Supplementary Methods). In addition, the copy

numbers of ammonia monooxygenase gene (*amoA*) of chemoautotrophic ammonia-oxidizing bacteria (AOB) and ammonia-oxidizing archaea (AOA) were also quantified. Q-PCR procedures were conducted on the ABI7500 Sequence detection system (Applied Biosystems, Canada). In this study, qPCR results with one melting-curve peak, amplification efficiencies higher than 90%, and correlation coefficients above 0.98 were employed. Details about the primer sequences and amplification conditions are presented in Table S3.

2.5 Metagenome sequencing and analysis

Total genomic DNA was paired-end sequenced with NovaSeq Reagent Kits on Illumina NovaSeq (Illumina Inc., San Diego, CA, USA) offered by Majorbio (Shanghai, China). Metagenomic data were analyzed on the online platform of Majorbio Cloud Platform (www.majorbio.com) (Ren et al., 2022). Raw reads were trimmed with fastp (v0.19.7) to eliminate low-quality reads and adaptors (https://github.com/OpenGene/fastp). The trimmed sequences were de novo assembled with MEGAHIT (https://github.com/voutcn/megahit) (Li et al., 2015). The obtained sequences were operated to predict open reading frame (ORF) with MetaGene (http://metagene.cb.k.u-tokyo.ac.jp/) (Noguchi et al., 2006) and construct a nonredundant gene catalog with CD-HIT (http://www.bioinformatics.org/cd-hit/) (Fu et al., 2012). SOAPaligner software (http://soap.genomics.org.cn/) was used to align

high-quality reads of each sample with non-redundant gene sets (default parameter: 95% identity), and the abundance information of genes in the corresponding samples was counted (Li et al., 2009). Finally, the representative sequences were categorized as taxonomy by comparing with the National Center for Biotechnology Information (NCBI) Non-Redundant Protein Sequence (NR) database and annotated biological functions by comparing with the Kyoto Encyclopedia of Genes and Genomes (KEGG) database at 1e-5 e-value cutoff using DIAMOND (https://github.com/bbuchfink/diamond) (Buchfink et al., 2015; Buchfink et al., 2021).

2.6 Statistical analysis

The change of DCF rate with warming was simulated by polynomial fitting using Origin software (Origin 2022). Pearson's correlation analysis was performed using Origin 2022. Principal coordinates analysis (PCoA) was performed to reveal the similarity and otherness of the estuarine and coastal water communities through R package. One-way analysis of variance (ANOVA) was conducted to investigate spatial variations in the optimum temperature (T_{opt}) of DCF processes (SPSS, version 25.0). $P<0.05$ was considered statistically significant.

3. Results

3.1 Chemoautotrophic microbes along the estuarine and coastal gradient

Community dynamics of chemoautotrophic microorganisms in the Yangtze Estuary and its adjacent coastal waters were explored via metagenomic analyses (Figure 2). Generally, the relative abundance of DCF microbes in the low salinity estuarine waters was lower than that in the middle and high salinity coastal areas (P<0.05) (Figure 2a). In addition, chemoautotrophic carbon fixation pathways varied significantly along the environmental gradient of the Yangtze Estuary and its adjacent coastal waters (Figures S1 and S2). CBB cycle was the dominant chemoautotrophic carbon fixation pathway at the low and middle salinity sites (S1-S4), while DCF at the high salinity sites was co-dominated by CBB and 3-HP/4-HB cycles (Figure 2a). Microbes performing CBB cycle were mainly affiliated to *Gammaproteobacteria* (22.1%) and *Betaproteobacteria* (19.2%), which were the dominant phylum in the middle-salinity and low-salinity areas, respectively (Figure 2b). The relative importance of 3-HP/4-HB cycle gradually increased from the upper estuary to the offshore areas, which was consistent with the abundance of *accA* gene (encoding the alpha subunit of acetyl-CoA carboxylase in 3-HP/4-HB cycle) based on Q-PCR results (P<0.05) (Figure 2c). Moreover, the abundance of *hbd* gene encoding 4-hydroxybutyryl-CoA dehydratase of 3-HP/4-HB cycle also tended to be higher at the high salinity sites (Figure 2c). *Thaumarchaeota* occupied 98.1% of all chemoautotrophs conducting 3-HP/4-HB cycle

(Figure 2b), of which ammonia-oxidized archaea (*Nitrosomarinus* and *Nitrosopelagicus*) were the dominant chemoautotrophs for DCF in the middle and high salinity waters (S3-S6) (Figure S3). However, in the low salinity estuarine waters (S1-S2), *Nitrospira*, which performs rTCA cycle and is mainly involved in the oxidation of nitrite, was the most important DCF genus (Figure S3). Generally, the relative importance of rTCA carbon fixation pathway decreased from the upper estuary to saline seawaters (Figure 2a), which was consistent with the Q-PCR result that the abundance of gene encoding the beta subunit of the ATP citrate lyase (*aclB*) in rTCA cycle was significantly higher at the low salinity sites (P<0.01) (Figure 2c). Furthermore, WL pathway mainly existed at the middle salinity sites (Figure 2a) with the maximal biodiversity of DCF microbes (Table S5). Nevertheless, 3-HP bicycle was even-distributed along the environmental gradient of the Yangtze Estuary, with most of the chemoautotrophs affiliating to *Alphaproteobacteria* (35.9%), *Actinobacteria* (34.2%) and *Gammaproteobacteria* (24.0%) (Figure 2a and 2b).

3.2 Response of DCF rates to temperature

Within the temperature range of 5 to 40 °C, DCF rates varied from 0.05 to 0.72 μmol C L^{-1} day^{-1} and showed a dome-shaped thermal response pattern (Figure 3). On the basis of the constructed temperature-response curves (Figure 3), the T_{opt} for DCF was estimated. DCF rates increased with temperature until the T_{opt} was reached, and

then decreased with further increment of temperature. Along the Yangtze estuarine and coastal gradient, the T_{opt} ranged from about 21.9 to 32.0 °C, which was significantly lower at the offshore sites (S5-S6) than at the nearshore sites (S1-S4) (one-way ANOVA, $P<0.05$). It should be noted that the minimal T_{opt} value (21.9 °C) was observed at the most offshore site S6, indicating that dark carbon fixation might be more vulnerable in saline seawater under the stress of global warming. The T_{opt} of nearshore sites (S1-S4) was higher than the current temperature (6-27.9 °C), and thus DCF rates mainly presented an increased trend with global warming. Nevertheless, the T_{opt} of offshore stations (S5-S6) was below the current temperature at part of the year, which leads to a decrease of DCF rates with the increase of temperature, especially in summer (Figure 3).

3.3 DCF capacity under different warming scenarios

The global sea surface temperature is estimated to increase by approximately 1.8 °C and 3.4 °C under the SSP2-4.5 and SSP5-8.5 scenarios, respectively, at the end of the 21st century relative to the recent reference period 1995-2014 (IPCC, 2021). Compared with the open ocean, estuaries are generally subjected to greater warming trends (Scanes et al., 2020). Therefore, in this study, 2 °C and 4 °C warming scenarios were assumed to evaluate the influence of global warming on DCF capacity in estuarine and coastal waters (Figures 4 and 5). The increase of temperature under these warming

scenarios apparently inhibited DCF rates in summer (except site S4) (Figure 4). Especially at the high salinity offshore sites (S5-S6), warming in August would inhibit DCF rates by 2.1-4.1% and 5.3-9.4% under the 2 °C and 4 °C warming scenarios, respectively. However, the inhibition of DCF rates by warming in summer was relatively lower at the lower salinity nearshore sites (S1-S3), with the inhibition of 0.7-1.2% and 2.2-3.6% in August under the 2 °C and 4 °C warming scenarios, respectively. In addition, the duration of warming inhibition was longer at the offshore sites than at the nearshore sites. Particularly, the duration of DCF inhibition at site S6 lasted from June to October (Figure 5). In contrast, warming in cooler seasons would promote DCF rates in estuarine and coastal waters, with a maximal stimulation occurring in February (24.0-113.9%) under 4 °C warming scenario. In addition, the promotion level of DCF rate by warming was higher at the nearshore sites than at the offshore sites (Figures 4 and 5). Under the 4 °C warming scenario, DCF rate might averagely increase by 19.3% in the nearshore area, while it would rise only by 8.8% in the offshore area (Figure 6). Generally, the annual DCF capacity of the whole Yangtze estuarine and coastal waters would increase by approximately 8.6% and 15.8% by 2100 under the 2 °C and 4 °C warming scenarios, respectively (Figure S4).

4. Discussion

As an important link converting inorganic carbon to organic matter, DCF is

regarded as an indispensable process in the global carbon cycle (Hügler & Sievert, 2010). Due to the widespread existence of chemoautotrophic microorganisms, DCF process is a significant carbon sink in dark ocean (Pachiadaki et al., 2017), hydrothermal vents (Nakagawa & Takai, 2008), and cold springs (Camacho et al., 2005). Estuaries and coasts are complex hydrodynamic ecosystems under the interaction between riverine runoff and tidal oscillation, which generally harbor high primary productivity and are important sources of organic matter and energy for adjacent oceanic areas (Signori et al., 2017). The importance of DCF in the biogeochemical cycle of carbon has been confirmed in estuarine and coastal ecosystems (Signori et al., 2017). However, the potential response of chemoautotrophic activities to climate warming in estuarine and coastal waters remains under exploration. In this study, the thermal response patterns of DCF rates in the Yangtze Estuary were investigated along the estuarine gradient. In addition, based on metagenome analyses, this study further revealed the molecular mechanisms of how chemoautotrophic microbial communities and carbon sequestration pathways regulate the thermal response of DCF in estuarine and coastal waters.

DCF rates in the Yangtze Estuary and its adjacent coastal waters were comparable to those reported in the Columbia River's Estuary (0.9-1.4 μmol C L^{-1} day^{-1}) (Bräuer et al., 2013) and a tropical estuarine system (0.4-1.3 μmol C L^{-1} day^{-1}) (Signori et al., 2017), but significantly higher than those detected in seawaters such as the North

Atlantic (3.0×10^{-5}-1.0×10^{-2} μmol C L^{-1} day^{-1}) (Pachiadaki et al., 2017) and the Arabian Sea (5.0×10^{-4}-1.2×10^{-2} μmol C L^{-1} day^{-1}) (Saxena et al., 2022). Compared with freshwater ecosystems, DCF rates measured in the Yangtze estuarine and coastal waters were significantly higher than those reported in deep groundwater of Sweden (3.9×10^{-3}-1.9×10^{-2} μmol C L^{-1} day^{-1}) (Overholt et al., 2022) and in the Maggiore Lake (1.3×10^{-2}-2.1×10^{-2} μmol C L^{-1} day^{-1}) (Callieri et al., 2014). Temperature is suggested to significantly affect the activity and abundance of microorganisms, thereby regulating DCF rate (Liu et al., 2022). In light of present and future anthropogenic-driven changes in climate, there is a rising interest for exploring the response of chemoautotrophic carbon fixation to temperature, as temperature change may have the potential to severely impact microbial performance and consequently ecosystem functioning (Alster et al., 2018). In this study, the response of DCF rate to temperature showed that below the optimum temperature, DCF rate increased spontaneously with the temperature rising constantly, while it dropped sharply when the temperature exceeds the T_{opt}. This response pattern may be explained by the intrinsic temperature sensitivity of enzymatic reactions (Brzostek & Finzi, 2012), since temperature can alter the biochemical kinetics and structural stability of enzymes (Somero, 2004). Generally, increasing temperature promotes catalytic rate, and DCF is thus enhanced due to increasing kinetic energy of reactants and rates of collision, as well as higher structural flexibility of enzymes (Davidson et al., 2006). However, excessive structural flexibility

can also lead to reduced ligand recognition and binding ability at active sites, thereby reducing kinetic efficiency and thus decreasing DCF rates (Zheng et al., 2020).

In the estuarine and coastal waters, significantly lower T_{opt} for DCF was observed at the offshore sites than at the nearshore sites (one-way ANOVA, $P<0.05$), which suggests that DCF at the offshore sites may be more vulnerable to temperature changes. Specifically, the DCF-promoting temperature rising limit was 6.3 °C higher at the nearshore sites than at the offshore sites (Figure 6), and the offshore sites were more significantly inhibited than the nearshore sites in warm seasons (Figure S5). Overall, the promotion level of annual DCF by warming was higher in the nearshore area than that in the offshore area (Figure 6). The higher vulnerability of DCF in high salinity offshore seawaters indicates that chemoautotrophic carbon fixation in the open oceans may also be sensitive to global warming, which needs to be investigated in future studies. The observed differences in thermal response were likely due to the spatial heterogeneity of chemoautotrophic microbial communities (Alster et al., 2018). It was reported that the difference in microbial physiology and kinetics among microbial communities may be important drivers of different temperature sensitivities (Alster et al., 2016; Alster et al., 2018). In this study, significant variations of chemoautotrophic microbial communities were detected along the Yangtze estuarine and coastal gradient (Figure 2), and the enzymes produced by different chemoautotrophs can vary in their temperature sensitivity, thus resulting in different carbon fixation kinetics among

sampling sites. In addition, it was observed that chemoautotrophs showed higher dependence on other microbes in high salinity offshore areas (Figure S6), which may lead to their vulnerability to temperature rise. Furthermore, environmental parameters may also influence the thermal response pattern of chemoautotrophs, but T_{opt} was only observed to be negatively correlated with DIC (P<0.05) across the Yangtze Estuary (Table S10). It is worth noting that the potential seasonal variations of microbial communities were not considered in the present study, which requires further refinement.

It was previously reported that, as temperature changes, the specific substrate affinity (α) of AOB-dominated estuarine waters varied in a narrower range relative to that of AOA-dominated coastal waters (Zheng et al., 2020), which reflects that AOB cope better with variable temperature. In contrast, AOA are more sensitive to temperature change and so may not be favored in a warming habitat. These hypotheses were confirmed in the present study, which showed higher T_{opt} at the AOB-dominated nearshore sites (26.8-32 °C) than at the AOA-dominated offshore sites (21.9-25.2 °C) (Figure 3). Especially, the T_{opt} for DCF at the offshore site S5 was around 25.2 °C, consistent with a reported value for an AOA isolate from laboratory culture (Qin et al., 2014). Meanwhile, the average T_{opt} of 28.3 °C at the nearshore sites was close to the range of 29-35 °C reported for AOB pure cultures (Groeneweg et al., 1994) (Figure 3). These results suggest that ammonia oxidizers may play an important role in

chemoautotrophic carbon fixation in estuarine and coastal waters. Consistently, nitrifiers were reported to be the major contributors to DCF in the dark ocean (Guerrero-Feijoo et al., 2018). Middelburg (2011) also showed that globally about 52% of the chemoautotrophic carbon fixation occurs by nitrifiers in the ocean water column. Moreover, Baltar et al. (2016) reported that chemoautotrophic ammonia oxidizing microorganisms were the main group responsible for the increased DIC fixation rates, which provided direct experimental evidence for ammonia as an important energy source for prokaryotic DIC fixation in the dark ocean. Furthermore, DCF rates were observed to be significantly promoted by NH_4^+ addition ($P<0.05$) in the present study (Supplementary Methods), further demonstrating that nitrifiers may play an important role in driving DCF (Figure S7). Among the ammonia oxidizers, AOA affiliated to *Thaumarchaeota*, immobilize CO_2 through 3-HP/4-HB cycle and are considered to be the dominant microbial group for ammonia oxidation and DCF in marine environments (Cao et al., 2012; Hansman et al., 2009; Herndl et al., 2005; Tetu et al., 2013; Walker et al., 2010). In the present study, *Thaumarchaeota* were also the dominant DCF microbes in the offshore waters, among which *Nitrosomarinus* and *Nitrosopelagicus* were the dominant genera, indicating the prominent contribution of AOA to DCF in the high salinity coastal waters. However, in the lower salinity nearshore waters, *Nitrospira* may play a more important role in DCF through rTCA cycle. Recent studies have also confirmed the role of NOB and comammox bacteria in DCF process at freshwater lakes

(Alfreider et al., 2018; Reinthaler et al., 2010). Therefore, nitrifiers play an important role in DCF and associated thermal response via occupying different ecological niches in estuarine and coastal waters.

It is interesting to find that the relative importance of WL pathway, the largest carbon fixation pathway in anaerobic conditions (Berg, 2011), was significantly higher in the middle-salinity zone than in the low-salinity and high-salinity waters (P<0.01) (Figure 2a), which is presumably related to the anaerobic microzone formed by microorganisms attached to the surface of suspended particles in the turbidity maximum zone (TMZ) (Zheng et al., 2021). Estuarine TMZ is characterized by a higher concentration of suspended particles than upstream or downstream zones, which is formed due to extensive interactions between land and sea and is prevalent in most estuaries around the world (Mitchell, 2013; Shen et al., 2008). The low-oxygen microsites around suspended particles in the TMZ waters can provide circumstances for anaerobic microbes (Jia et al., 2016; Zheng et al., 2021), as well as those performing DCF through the WL pathway. In the Yangtze Estuary and its adjacent coastal waters, anaerobic microorganisms conducting DCF via WL, most of which were affiliated to the phylum *Chloroflexi*, *Deltaproteobacteria*, *Armatimonadetes*, *Actinobacteria* and *Planctomycetes*, were found to be enriched in the TMZ waters (Figure 2b). In addition, higher DCF microbial diversity was likely resulted from the extensive material exchanges between land and sea in these middle-salinity TMZ waters (Table S5) (Zheng

et al., 2021).

In summary, the thermal response pattern of DCF in estuarine and coastal waters was first investigated, and the potential DCF changes under different warming scenarios were predicted. DCF rate in estuarine and coastal ecosystems was highly temperature-dependent, and DCF was more susceptible to warming at the offshore sites than at the nearshore sites. Future warming would possibly suppress DCF in summer and fall, while stimulating DCF in winter and spring. Under 2 °C warming scenario, the annual DCF in the Yangtze Estuary and its adjacent coastal waters was estimated to averagely increase by 8.6% by 2100. Metagenome analyses further revealed that nitrifiers play a significant role in mediating DCF process in estuarine and coastal waters. This study provides important insights about the chemoautotrophic carbon sink in estuarine and coastal waters under the context of global warming.

Author Contributions

Y.L.Z., L.J.H., L.Q. and B.L.L. designed the study. L.Q., B.L.L. and J.Z. collected data. L.Q, B.L.L., Y.L.Z., Z.R.A., J.Z., L.W., F.Y.C., Z.K.L., G.Y.Y., H.P.D. and X.F.L. performed the analysis and prepared the paper materials. All authors participated in discussions about data interpretation. L.Q., Y.L.Z. and L.J.H. wrote the manuscript. Funding that supported this study was obtained by Y.L.Z., L.J.H. and M.L.

Notes

The authors declare no potential conflicts of interest.

Acknowledgements

This work is supported by the National Natural Science Foundation of China (Nos. 42030411, 41971105, 42222605, 42230505, 41725002, and 41730646), the Chinese National Key Programs for Fundamental Research and Development (Nos. 2016YFA0600904), and Director's Fund of Key Laboratory of Geographic Information Science (Ministry of Education), East China Normal University (Grant No. KLGIS2022C03).

Data Availability Statement

The sequence data that support the findings of this study are openly available in National Center for Biotechnology Information (NCBI) Sequence Read Archive (SRA) database under BioProject accession number PRJNA923751 (https://www.ncbi.nlm.nih.gov/bioproject/PRJNA923751), and all other data needed to evaluate the conclusions are available in DYRAD (https://doi.org/10.5061/dryad.37pvmcvqf).

References

Alfreider, A., Baumer, A., Bogensperger, T., Posch, T., Salcher, M. M., & Summerer, M. (2017). CO_2 assimilation strategies in stratified lakes: Diversity and distribution patterns of chemolithoautotrophs. *Environmental Microbiology*, 19(7), 2754-2768. https://doi.org/10.1111/1462-2920.13786

Alfreider, A., Grimus, V., Luger, M., Ekblad, A., Salcher, M. M., & Summerer, M. (2018). Autotrophic carbon fixation strategies used by nitrifying prokaryotes in freshwater lakes. *FEMS Microbiology Ecology*, 94(10), fiy163. https://doi.org/10.1093/femsec/fiy163

Alonso-Saez, L., Galand, P. E., Casamayor, E. O., Pedros-Alio, C., & Bertilsson, S. (2010). High bicarbonate assimilation in the dark by Arctic bacteria. *Isme Journal*, 4(12), 1581-1590. https://doi.org/10.1038/ismej.2010.69

Alster, C. J., Koyama, A., Johnson, N. G., Wallenstein, M. D., & von Fischer, J. C. (2016). Temperature sensitivity of soil microbial communities: An application of macromolecular rate theory to microbial respiration. *Journal of Geophysical Research: Biogeosciences*, 121(6), 1420-1433. https://doi.org/10.1002/2016JG003343

Alster, C. J., Weller, Z. D., & von Fischer, J. C. (2018). A meta-analysis of temperature sensitivity as a microbial trait. *Global Change Biology*, 24(9), 4211-4224. https://doi.org/10.1111/gcb.14342

Baltar, F., Lundin, D., Palovaara, J., Lekunberri, I., Reinthaler, T., Herndl, G. J., & Pinhassi, J. (2016). Prokaryotic responses to ammonium and organic carbon reveal alternative CO_2 fixation pathways and importance of alkaline phosphatase in the mesopelagic North Atlantic. *Frontiers in Microbiology*, 7, 1670. https://doi.org/10.3389/fmicb.2016.01670

Bar-Even, A., Noor, E., & Milo, R. (2012). A survey of carbon fixation pathways through a quantitative lens. *Journal of Experimental Botany,* 63(6), 2325-2342. https://doi.org/10.1093/jxb/err417

Belkin, I. M. (2009). Rapid warming of Large Marine Ecosystems. *Progress in Oceanography*, 81(1), 207-213. https://doi.org/10.1016/j.pocean.2009.04.011

Berg, I. A. (2011). Ecological aspects of the distribution of different autotrophic CO_2 fixation pathways. *Applied and Environmental Microbiology*, 77(6), 1925-1936. https://doi.org/10.1128/AEM.02473-10

Bräuer, S. L., Kranzler, K., Goodson, N., Murphy, D., Simon, H. M., Baptista, A. M., & Tebo, B. M. (2013). Dark carbon fixation in the Columbia River's estuarine turbidity maxima: Molecular characterization of red-type *cbbL* genes and measurement of DIC uptake rates in response to added electron donors. *Estuaries and Coasts*, 36(5), 1073-1083. https://doi.org/10.1007/s12237-013-9603-6

Brzostek, E. R., & Finzi, A. C. (2012). Seasonal variation in the temperature sensitivity

of proteolytic enzyme activity in temperate forest soils. *Journal of Geophysical Research: Biogeosciences*, 117(G1). https://doi.org/10.1029/2011JG001688

Buchfink, B., Reuter, K., & Drost, H.-G. (2021). Sensitive protein alignments at tree-of-life scale using DIAMOND. *Nature Methods*, 18(4), 366-368. https://doi.org/10.1038/s41592-021-01101-x

Buchfink, B., Xie, C., & Huson, D. H. (2015). Fast and sensitive protein alignment using DIAMOND. *Nature Methods*, 12(1), 59-60. https://doi.org/10.1038/nmeth.3176

Callieri, C., Coci, M., Eckert, E. M., Salcher, M. M., & Bertoni, R. (2014). Archaea and Bacteria in deep lake hypolimnion: in situ dark inorganic carbon uptake. *Journal of Limnology*, 73(1), 47-54. https://doi.org/10.4081/jlimnol.2014.937

Camacho, A., Rochera, C., Silvestre, J. J., Vicente, E., & Hahn, M. W. (2005). Spatial dominance and inorganic carbon assimilation by conspicuous autotrophic biofilms in a physical and chemical gradient of a cold sulfurous spring: The role of differential ecological strategies. *Microbial Ecology*, 50(2), 172-184. https://doi.org/10.1007/s00248-004-0156-x

Cao, H., Hong, Y., Li, M., & Gu, J.-D. (2012). Community shift of ammonia-oxidizing bacteria along an anthropogenic pollution gradient from the Pearl River Delta to the South China Sea. *Applied Microbiology and Biotechnology*, 94(1), 247-259. https://doi.org/10.1007/s00253-011-3636-1

Davidson, E. A., Janssens, I. A., & Luo, Y. (2006). On the variability of respiration in terrestrial ecosystems: moving beyond Q_{10}. *Global Change Biology*, 12(2), 154-164. https://doi.org/10.1111/j.1365-2486.2005.01065.x

Figueroa, I. A., Barnum, T. P., Somasekhar, P. Y., Carlstrom, C. I., Engelbrektson, A. L., & Coates, J. D. (2018). Metagenomics-guided analysis of microbial chemolithoautotrophic phosphite oxidation yields evidence of a seventh natural CO_2 fixation pathway. *Proceedings of the National Academy of Sciences*, 115(1), E92-E101. https://doi.org/10.1073/pnas.1715549114

Fu, L., Niu, B., Zhu, Z., Wu, S., & Li, W. (2012). CD-HIT: Accelerated for clustering the next-generation sequencing data. *Bioinformatics*, 28(23), 3150-3152. https://doi.org/10.1093/bioinformatics/bts565

Garcia-Cantizano, J., Casamayor, E. O., Gasol, J. M., Guerrero, R., & Pedros-Alio, C. (2005). Partitioning of CO_2 incorporation among planktonic microbial guilds and estimation of in situ specific growth rates. *Microbial Ecology*, 50(2), 230-241. https://doi.org/10.1007/s00248-004-0144-9

Giese, M. (1994). Joint Global Ocean Flux Study (JGOFS). *Environmental Science and Pollution Research*, 1(3), 177-177. https://doi.org/10.1007/BF02986941

Groeneweg, J., Sellner, B., & Tappe, W. (1994). Ammonia oxidation in *Nitrosomonas* at NH_3 concentrations near K_m: Effects of pH and temperature. *Water Research*, 28(12), 2561-2566. https://doi.org/10.1016/0043-1354(94)90074-4

Guerrero-Feijoo, E., Sintes, E., Herndl, G. J., & Varela, M. M. (2018). High dark inorganic carbon fixation rates by specific microbial groups in the Atlantic off the Galician coast (NW Iberian margin). *Environment Microbiology*, 20(2), 602-611. https://doi.org/10.1111/1462-2920.13984

Hansman, R. L., Griffin, S., Watson, J. T., Druffel, E. R. M., Ingalls, A. E., Pearson, A., & Aluwihare, L. I. (2009). The radiocarbon signature of microorganisms in the mesopelagic ocean. *Proceedings of the National Academy of Sciences*, 106(16), 6513-6518. https://doi.org/10.1073/pnas.0810871106

Herndl, G. J., Reinthaler, T., Teira, E., van Aken, H., Veth, C., Pernthaler, A., & Pernthaler, J. (2005). Contribution of Archaea to total prokaryotic production in the deep Atlantic Ocean. *Applied and Environmental Microbiology*, 71(5), 2303-2309. https://doi.org/10.1128/AEM.71.5.2303-2309.2005

Hügler, M., & Sievert, S. M. (2010). Beyond the Calvin cycle: Autotrophic carbon fixation in the ocean. *Annual Review of Marine Science*, 3(1), 261-289. https://doi.org/10.1146/annurev-marine-120709-142712

IPCC. (2021) Summary for policymakers Climate Change 2021: The Physical Science Basis Contribution of Working Group I to the Sixth Assessment Report of the Intergovernmental Panel on Climate Change ed Masson-Delmotte, V., Zhai, P., Pirani, A., Connors, S. L., Péan, C., Berger, S., Caud, N., Chen, Y., Goldfarb, L., Gomis, M. I., Huang, M., Leitzell, K., Lonnoy, E., Matthews, J.B.R., Maycock,

T. K., Waterfield, T., Yelekçi, O., Yu, R., & Zhou, B. Cambridge University Press.

Jia, Z., Liu, T., Xia, X., & Xia, N. (2016). Effect of particle size and composition of suspended sediment on denitrification in river water. *Science of The Total Environment*, 541, 934-940. https://doi.org/10.1016/j.scitotenv.2015.10.012

Jørgensen, B. B. (1982). Mineralization of organic matter in the sea bed-the role of sulphate reduction. *Nature*, 296, 643-645. https://doi.org/10.1038/296643a0

Kyewalyanga, M. S., Naik, R., Hegde, S., Raman, M., Barlow, R., & Roberts, M. (2007). Phytoplankton biomass and primary production in Delagoa Bight Mozambique: Application of remote sensing. *Estuarine, Coastal and Shelf Science*, 74(3), 429-436. https://doi.org/10.1016/j.ecss.2007.04.027

Labrenz, M., Jost, G., Pohl, C., Beckmann, S., Martens-Habbena, W., & Jürgens, K. (2005). Impact of different in vitro electron donor/acceptor conditions on potential chemolithoautotrophic communities from marine pelagic redoxclines. *Applied and Environmental Microbiology*, 71(11), 6664-6672. https://doi.org/10.1128/AEM.71.11.6664-6672.2005

Li, D., Liu, C.-M., Luo, R., Sadakane, K., & Lam, T.-W. (2015). MEGAHIT: An ultra-fast single-node solution for large and complex metagenomics assembly via succinct de Bruijn graph. *Bioinformatics*, 31(10), 1674-1676. https://doi.org/10.1093/bioinformatics/btv033

Li, R., Yu, C., Li, Y., Lam, T.-W., Yiu, S.-M., Kristiansen, K., & Wang, J. (2009). SOAP2: An improved ultrafast tool for short read alignment. *Bioinformatics*, 25(15), 1966-1967. https://doi.org/10.1093/bioinformatics/btp336

Liu, B., Hou, L., Zheng, Y., Zhang, Z., Tang, X., Mao, T., Du, J., Bi, Q., Dong, H., Yin, G., Han, P., Liang, X., & Liu, M. (2022). Dark carbon fixation in intertidal sediments: Controlling factors and driving microorganisms. *Water Research*, 216, 118381. https://doi.org/10.1016/j.watres.2022.118381

Middelburg, J. J. (2011). Chemoautotrophy in the ocean. *Geophysical Research Letters*, 38(24). https://doi.org/10.1029/2011GL049725

Mitchell, S. B. (2013). Turbidity maxima in four macrotidal estuaries. *Ocean & Coastal Management*, 79, 62-69. https://doi.org/10.1016/j.ocecoaman.2012.05.030

Molari, M., Manini, E., Dell'Anno, A. (2013). Dark inorganic carbon fixation sustains the functioning of benthic deep-sea ecosystems. *Global Biogeochemical Cycles*, 27(1), 212-221. https://doi.org/10.1002/gbc.20030

Nakagawa, S., & Takai, K. (2008). Deep-sea vent chemoautotrophs: diversity, biochemistry and ecological significance. *FEMS Microbiology Ecology*, 65(1), 1-14. https://doi.org/10.1111/j.1574-6941.2008.00502.x

Noguchi, H., Park, J., & Takagi, T. (2006). MetaGene: Prokaryotic gene finding from environmental genome shotgun sequences. *Nucleic Acids Research*, 34(19), 5623-5630. https://doi.org/10.1093/nar/gkl723

Overholt, W. A., Trumbore, S., Xu, X., Bornemann, T. L. V., Probst, A. J., Krüger, M., Herrmann, M., Thamdrup, B., Bristow, L. A., Taubert, M., Schwab, V. F., Hölzer, M., Marz, M., & Küsel, K. (2022). Carbon fixation rates in groundwater similar to those in oligotrophic marine systems. *Nature Geoscience*, 15(7), 561-567. https://doi.org/10.1038/s41561-022-00968-5

Pachiadaki, M. G., Sintes, E., Bergauer, K., Brown, J. M., Record, N. R., Swan, B. K., Mathyer, M. E., Hallam, S. J., Lopez-Garcia, P., Takaki, Y., Nunoura, T., Woyke, T., Herndl, G. J., & Stepanauskas, R. (2017). Major role of nitrite-oxidizing bacteria in dark ocean carbon fixation. *Science*, 358(6366), 1046-1051. https://doi.org/10.1126/science.aan8260

Qin, W., Amin, S. A., Martens-Habbena, W., Walker, C. B., Urakawa, H., Devol, A. H., Ingalls, A. E., Moffett, J. W., Armbrust, E. V., & Stahl, D. A. (2014). Marine ammonia-oxidizing archaeal isolates display obligate mixotrophy and wide ecotypic variation. *Proceedings of the National Academy of Sciences*, 111(34), 12504-12509. https://doi.org/10.1073/pnas.1324115111

Reinthaler, T., van Aken, H. M., & Herndl, G. J. (2010). Major contribution of autotrophy to microbial carbon cycling in the deep North Atlantic's interior. *Deep Sea Research Part II: Topical Studies in Oceanography*, 57(16), 1572-1580. https://doi.org/10.1016/j.dsr2.2010.02.023

Ren, Y., Yu, G., Shi, C., Liu, L., Guo, Q., Han, C., Zhang, D., Zhang, L., Liu, B., Gao,

H., Zeng, J., Zhou, Y., Qiu, Y., Wei, J., Luo, Y., Zhu, F., Li, X., Wu, Q., Li, B., Fu, W., Tong, Y., Meng, J., Fang, Y., Dong, J., Feng, Y., Xie, S., Yang, Q., Yang, H., Wang, Y., Zhang, J., Gu, H., Xuan, H., Zou, G., Luo, C., Huang, L., Yang, B., Dong, Y., Zhao, J., Han, J., Zhang, X., & Huang, H. (2022). Majorbio Cloud: A one-stop, comprehensive bioinformatic platform for multiomics analyses. *iMeta*, 1(2), e12. https://doi.org/10.1002/imt2.12

Saxena, H., Sahoo, D., Nazirahmed, S., Rai, D. K., Khan, M. A., Sharma, N., Kumar, S., & Singh, A. (2022). Contribution of carbon fixation toward carbon sink in the ocean twilight zone. *Geophysical Research Letters*, 49(18), e2022GL099044. https://doi.org/10.1029/2022GL099044

Scanes, E., Scanes, P. R., & Ross, P. M. (2020). Climate change rapidly warms and acidifies Australian estuaries. *Nature Communications*, 11(1), 1803. https://doi.org/10.1038/s41467-020-15550-z

Scranton, M. I., Taylor, G. T., Thunell, R. C., Muller-Karger, F. E., Astor, Y., Swart, P., Edgcomb, V. P., & Pachiadaki, M. G. (2020). Anomalous $\delta^{13}C$ in particulate organic carbon at the chemoautotrophy maximum in the Cariaco Basin. *Journal of Geophysical Research: Biogeosciences*, 125(2), e2019JG005276. https://doi.org/10.1029/2019JG005276

Shen, Z., Zhou, S., & Pei, S. (2008). Transfer and transport of phosphorus and silica in the turbidity maximum zone of the Changjiang estuary. *Estuarine, Coastal and*

Shelf Science, 78(3), 481-492. https://doi.org/10.1016/j.ecss.2008.01.010

Signori, C. N., Valentin, J. L., Pollery, R. C. G., & Enrich-Prast, A. (2017). Temporal variability of dark carbon fixation and bacterial production and their relation with environmental factors in a tropical estuarine system. *Estuaries and Coasts*, 41(4), 1089-1101. https://doi.org/10.1007/s12237-017-0338-7

Somero, G. N. (2004). Adaptation of enzymes to temperature: searching for basic "strategies". *Comparative Biochemistry and Physiology Part B: Biochemistry and Molecular Biology*, 139(3), 321-333. https://doi.org/10.1016/j.cbpc.2004.05.003

Sun, Z., Chong, L., Meng, X., Hu, C., Zheng, J., & Gao, J. (2022). Multivariate relations of river habitat to water-sediment indexes in the Yangtze Estuary. *CATENA*, 216, 106416. https://doi.org/10.1016/j.catena.2022.106416

Takai, K., Campbell, B. J., Cary, S. C., Suzuki, M., Oida, H., Nunoura, T., Hirayama, H., Nakagawa, S., Suzuki, Y., Inagaki, F., & Horikoshi, K. (2005). Enzymatic and genetic characterization of carbon and energy metabolisms by deep-sea hydrothermal chemolithoautotrophic isolates of *Epsilonproteobacteria*. *Applied and Environmental Microbiology*, 71(11), 7310-7320. https://doi.org/10.1128/AEM.71.11.7310-7320

Tetu, S. G., Breakwell, K., Elbourne, L. D. H., Holmes, A. J., Gillings, M. R., & Paulsen, I. T. (2013). Life in the dark: metagenomic evidence that a microbial slime

community is driven by inorganic nitrogen metabolism. *ISME Journal*, 7(6), 1227-1236. https://doi.org/10.1038/ismej.2013.14

Walker, C. B., de la Torre, J. R., Klotz, M. G., Urakawa, H., Pinel, N., Arp, D. J., Brochier-Armanet, C., Chain, P. S. G., Chan, P. P., Gollabgir, A., Hemp, J., Hügler, M., Karr, E. A., Könneke, M., Shin, M., Lawton, T. J., Lowe, T., Martens-Habbena, W., Sayavedra-Soto, L. A., Lang, D., Sievert, S. M., Rosenzweig, A. C., Manning, G., & Stahl, D. A. (2010). *Nitrosopumilus maritimus* genome reveals unique mechanisms for nitrification and autotrophy in globally distributed marine crenarchaea. *Proceedings of the National Academy of Sciences*, 107(19), 8818–8823. https://doi.org/10.1073/pnas.0913533107

Walker, T. W. N., Kaiser, C., Strasser, F., Herbold, C. W., Leblans, N. I. W., Woebken, D., Janssens, I. A., Sigurdsson, B. D., & Richter, A. (2018). Microbial temperature sensitivity and biomass change explain soil carbon loss with warming. *Nature Climate Change*, 8(10), 885-889. https://doi.org/10.1038/s41558-018-0259-x

Wang, J., Wang, J., Xu, J., Yang, Y., Lyv, Y., & Luan, K. (2021). Seasonal and interannual variations of sea surface temperature and influencing factors in the Yangtze River Estuary. *Regional Studies in Marine Science*, 45, 101827. https://doi.org/10.1016/j.rsma.2021.101827

Yakimov, M. M., Cono, V. L., Smedile, F., DeLuca, T. H., Juárez, S., Ciordia, S., Fernández, M., Albar, J. P., Ferrer, M., Golyshin, P. N., & Giuliano, L. (2011). Contribution of crenarchaeal autotrophic ammonia oxidizers to the dark primary production in Tyrrhenian deep waters (Central Mediterranean Sea). *ISME Journal*, 5(6), 945-961. https://doi.org/10.1038/ismej.2010.197

Zheng, Y., Hou, L., Zhang, Z., Ge, J., Li, M., Yin, G., Han, P., Dong, H., Liang, X., Gao, J., Gao, D., & Liu, M. (2021). Overlooked contribution of water column to nitrogen removal in estuarine turbidity maximum zone (TMZ). *Science of The Total Environment*, 788, 147736. https://doi.org/10.1016/j.scitotenv.2021.147736

Zheng, Y., Jiang, X., Hou, L., Liu, M., Lin, X., Gao, J., Li, X., Yin, G., Yu, C., & Wang, R. (2016). Shifts in the community structure and activity of anaerobic ammonium oxidation bacteria along an estuarine salinity gradient. *Journal of Geophysical Research: Biogeosciences*, 121(6), 1632-1645. https://doi.org/10.1002/2015JG003300

Zheng, Z., Zheng, L., Xu, M. N., Tan, E., Hutchins, D. A., Deng, W., Zhang, Y., Shi, D., Dai, M., & Kao, S.-J. (2020). Substrate regulation leads to differential responses of microbial ammonia-oxidizing communities to ocean warming. *Nature Communications*, 11(1), 3511. https://doi.org/10.1038/s41467-020-17366-3

Zhou, W., Liao, J., Guo, Y., Yuan, X., Huang, H., Yuan, T., & Liu, S. (2017). High dark

carbon fixation in the tropical South China Sea. *Continental Shelf Research*, 146, 82-88. https://doi.org/10.1016/j.csr.2017.08.005

Figure Legends

Figure 1 Study area. Map shows the location of the Yangtze Estuary and the sampling stations. Blue areas and numbers indicate the isobath. Map lines delineate study areas and do not necessarily depict accepted national boundaries.

Figure 2 DCF microbial communities and abundance in the Yangtze Estuary and its adjacent coastal waters. (a) The relative abundance of different carbon fixation pathways based on KEGG function annotations. **(b)** Compositions of the DCF pathways at the phylum and class level based on KEGG function annotations. Coverages of these representative groups with different DCF pathways are given in Table S4. Different colors indicate different carbon fixation pathways. **(c)** Abundance of *cbbL* gene (i), *cbbM* gene (ii), *accA* gene (iii), *hbd* gene (iv), *aclB* gene (v), archaeal *amoA* and bacterial *amoA* gene (vi) based on Q-PCR. Error bar denotes the standard deviation (SD) (n=3).

Figure 3 Temperature dependence of DCF rate along the estuarine and coastal gradient. (a-d) Nearshore sites. **(e-f)** Offshore sites. DCF rates are shown as solid triangles. Error bars denote the standard deviation (SD) (n=3). Temperature response of DCF was fitted by polynomial curves. For all the lines, $P<0.05$. The 95% confidence intervals are described in light-colored regions. The optimum reaction temperatures (T_{opt}) are given in dotted lines. Equations and *P* values for the fitted curves are given in Table S6.

Figure 4 Effects of warming on DCF rates along the environmental gradient of the Yangtze Estuary and its adjacent coastal waters. (a) Under 2 °C warming scenario. **(b)** Under 4 °C warming scenario. For all the lines, $P<0.01$. Equations and P values for the fitted curves are given in Table S7.

Figure 5 Response of DCF rates under different warming scenarios in estuarine and coastal waters. (a) Increase of DCF rates under 2 °C and 4 °C warming scenarios in nearshore waters. **(b)** Increase of DCF rates under 2 °C and 4 °C warming scenarios in offshore waters. Sites with salinity lower than 30 are classified as nearshore sites (S1-S4), while those with salinity above 30 are classified as offshore sites (S5-S6). Data represent the average values of the DCF rate increase at nearshore or offshore sites. For all the lines, $P<0.001$. Equations and P values for the fitted curves are given in Table S8.

Figure 6 Warming-driven DCF promotion in the Yangtze estuarine and coastal waters. The shaded area represents a 4 °C increase in temperature. Sites with salinity lower than 30 are classified as nearshore sites (S1-S4), while those with salinity above 30 are classified as offshore sites (S5-S6). Data represent the average values of the DCF rate increase at nearshore or offshore sites. For all the lines, $P<0.001$. Equations and P values for the fitted curves are given in Table S9.

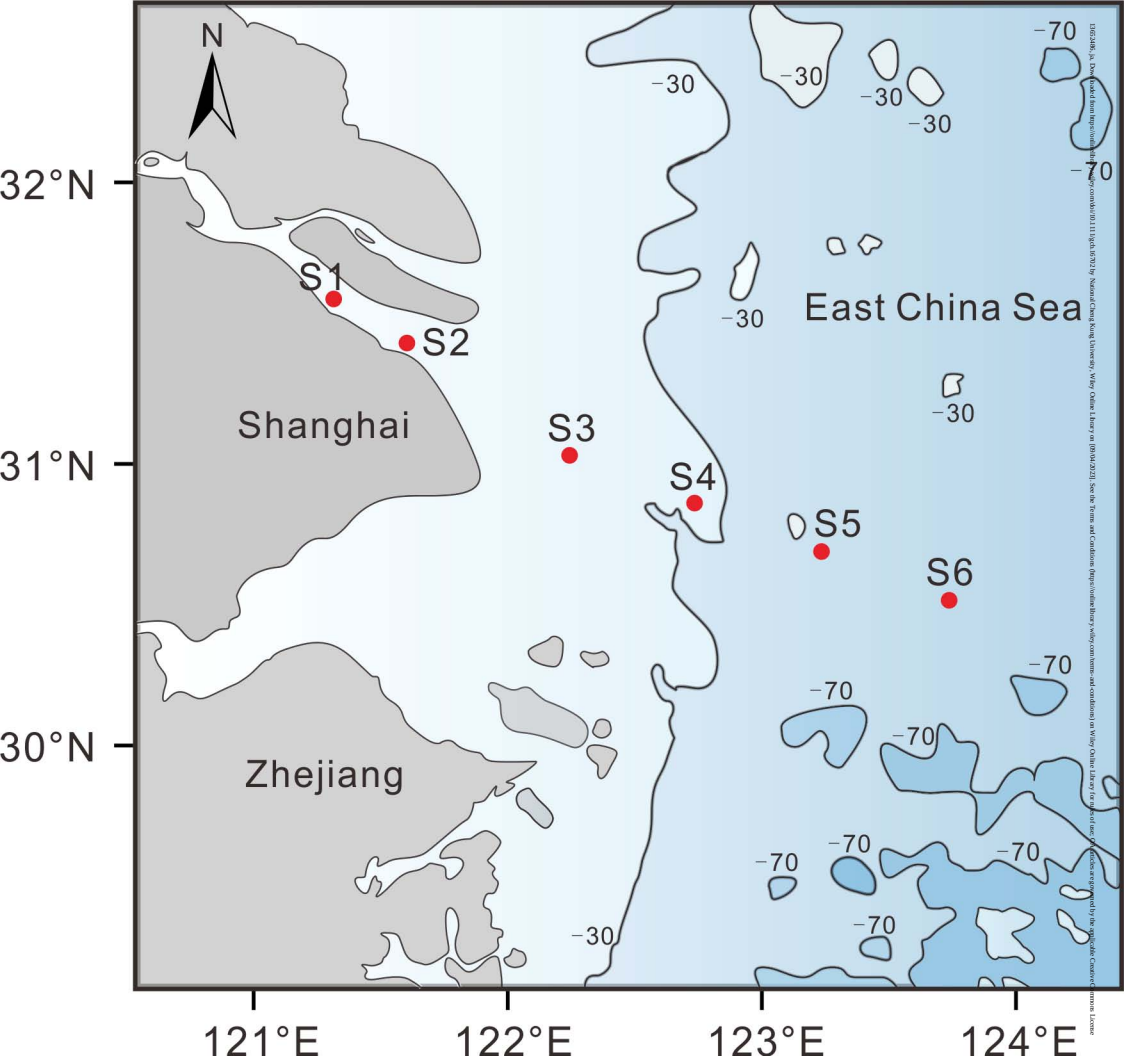
N
32°N
31°N
30°N
121°E
122°E
123°E
124°E
S1
S2
S3
S4
S5
S6
Shanghai
Zhejiang
East China Sea
-30
-70

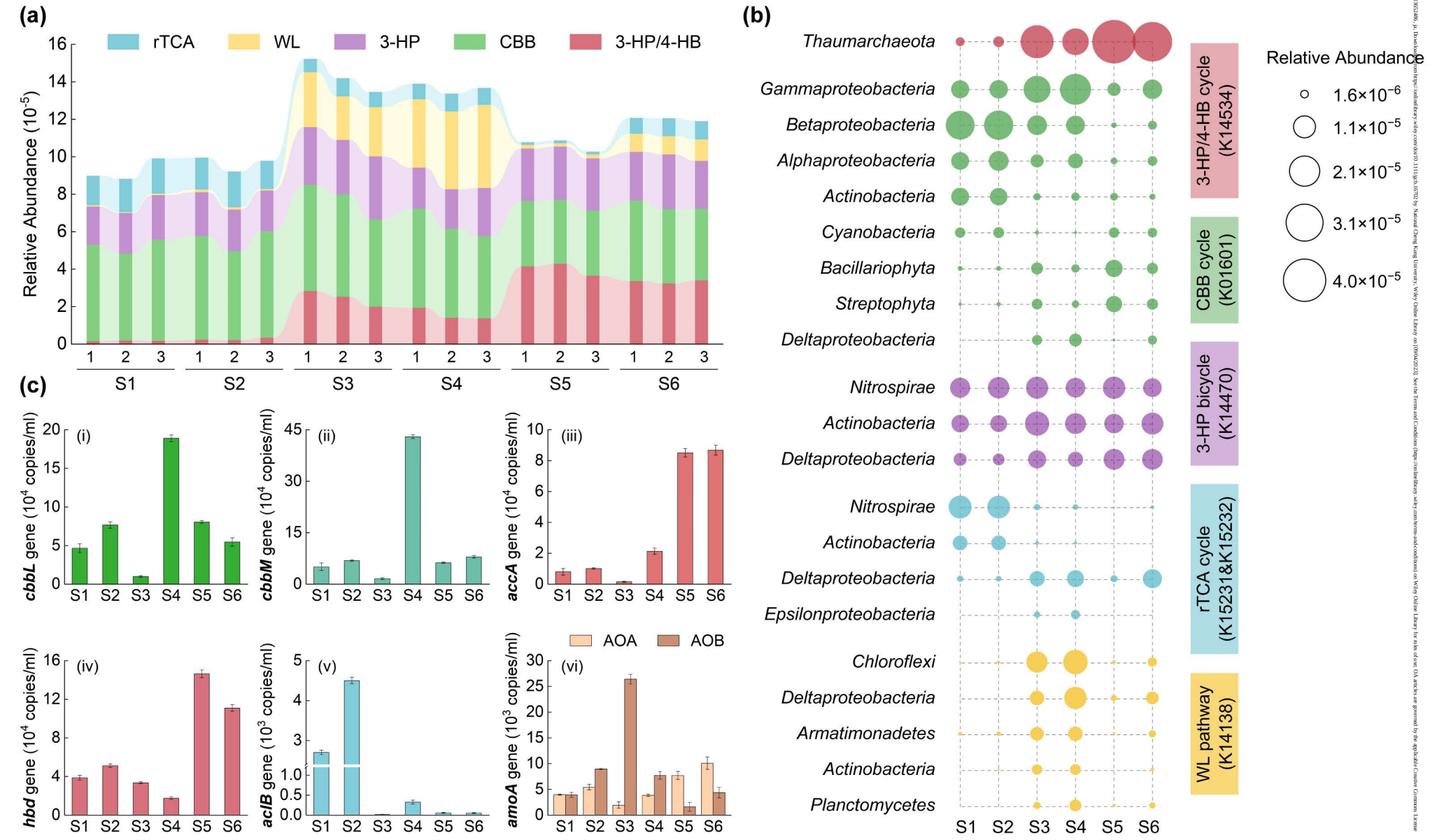

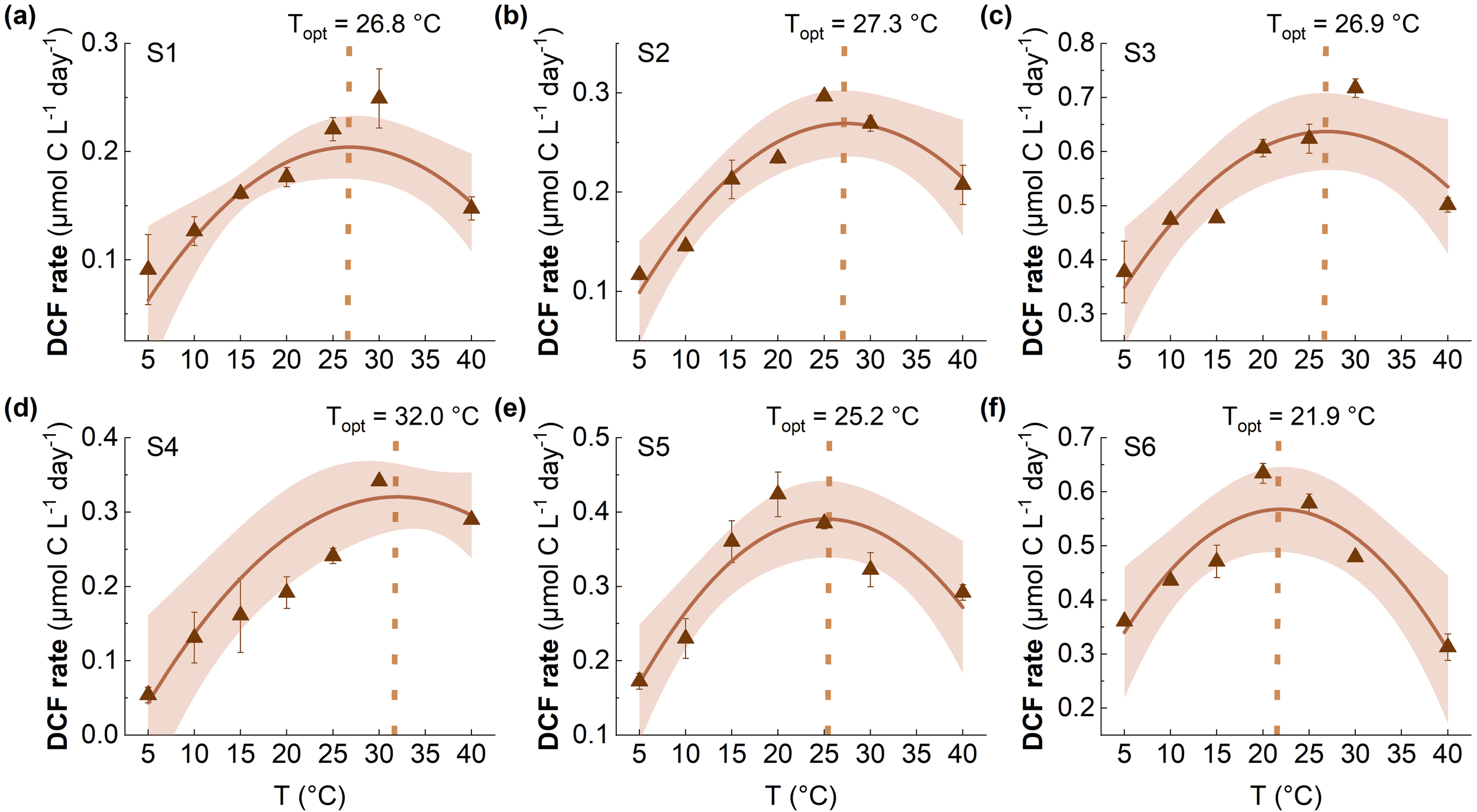

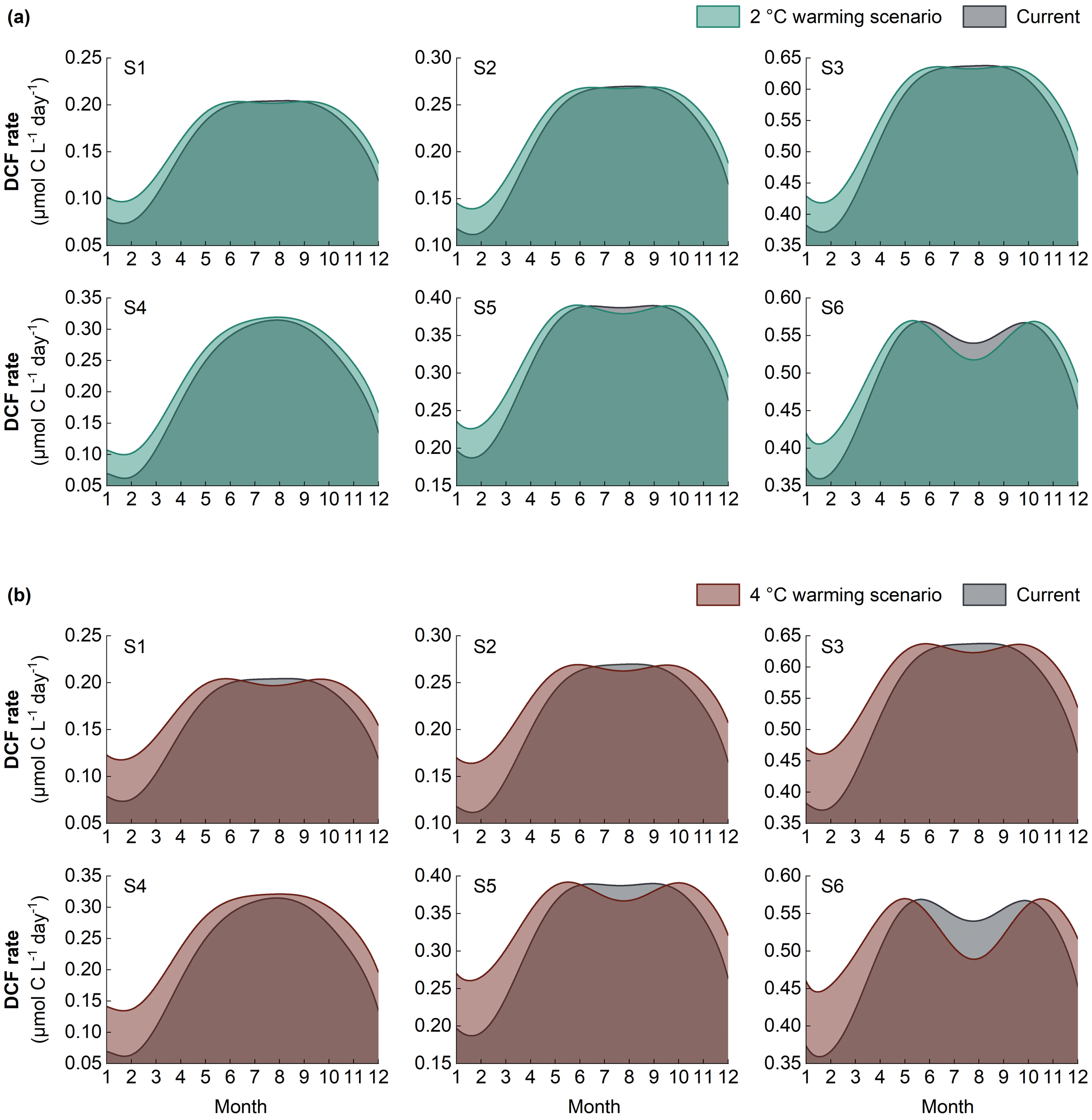

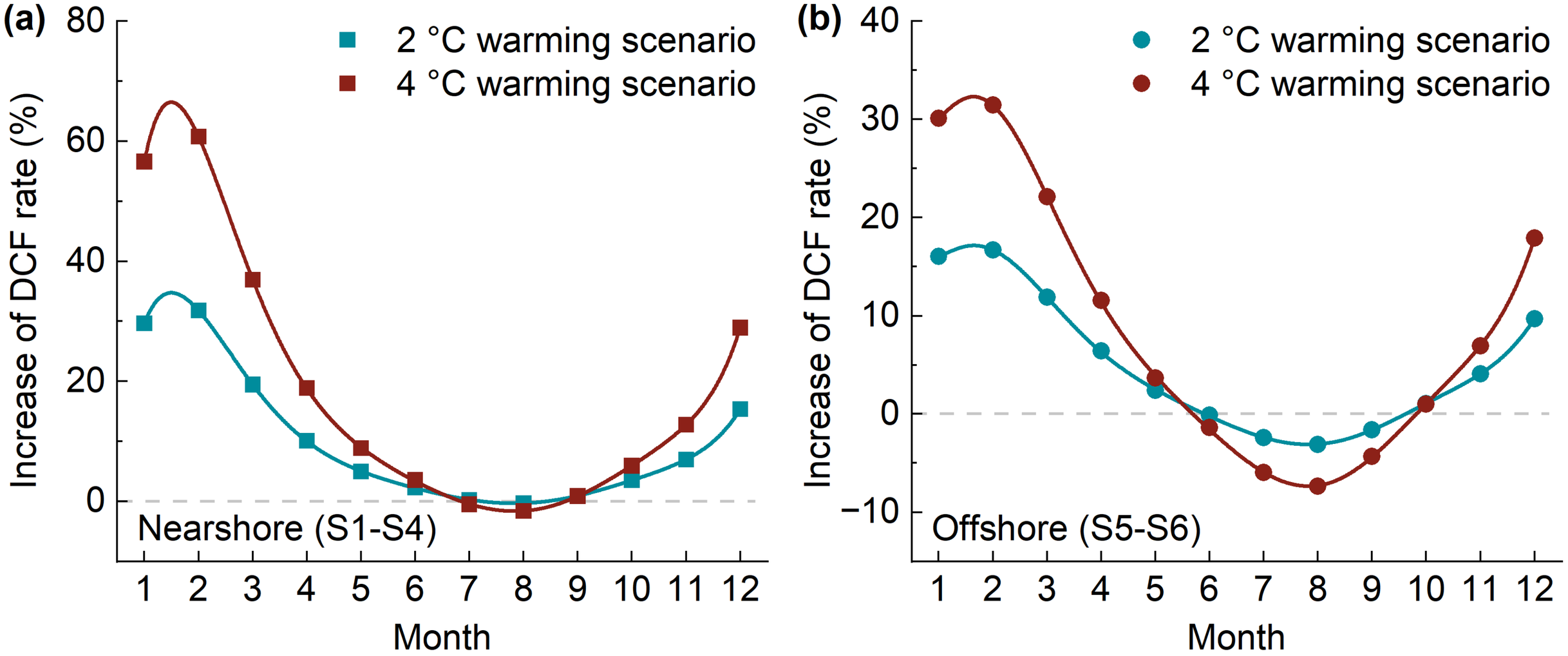
(a)
Increase of DCF rate (%)
80
60
40
20
0
2 °C warming scenario
4 °C warming scenario
Nearshore (S1-S4)
1 2 3 4 5 6 7 8 9 10 11 12
Month
(b)
Increase of DCF rate (%)
40
30
20
10
0
−10
2 °C warming scenario
4 °C warming scenario
Offshore (S5-S6)
1 2 3 4 5 6 7 8 9 10 11 12
Month